SI Materials and Methods

Microglial isolation from mouse brains. Microglia was isolated from the mouse cortex according to manufacturer protocol using anti-CD11b MACS beads (Mitenyl Biotech, 130-093-634) (1). Isolated cells were stained with anti-CD11b-FITC (BD Biosciences, M1/40, 553310), anti-CD45-PE (BD Biosciences, 30F-11, 553081), and anti-CD14-PE (BD Biosciences, rmC5-3, 553740) antibodies for one hour, and then subjected to a FACSCalibur flow cytometer (BD Biosciences). For some experiments, isolated cells were directly subjected to analysis using qRT-PCR.

RNA-sequencing, quality control and normalization. Mouse cortical samples were treated with TRIzol RNA Isolation Reagents (Thermo Fisher Scientific, 15596026), and total RNAs were subsequently extracted from samples using DNase (QIAGEN, 79254) and an RNeasy mini kit (QIAGEN, 74104). Additionally, the RNA integrity number (RIN) of total RNAs was measured with a 2100 Bioanalyzer (Agilent Technologies) using an RNA 6000 nano kit (Agilent Technologies, 5067-1511). Total RNAs were sequenced with Illumina HiSeq 4000 at the Mayo Clinic Genome Facility. Reads were mapped to the mouse genome mm10. Raw gene read counts, along with sequencing quality control, were generated using the Mayo Clinic RNA-sequencing analytic pipeline, MAP-RSeq Version 2.1.1 (2) In order to correct for GC bias and gene length differences and obtain similar quantile-by-quantile distributions of gene expression levels across samples, we performed conditional quantile normalization (CQN) was on the raw gene counts. According to the bimodal distribution of the CQN-normalized and $\log_2$-transformed reads per kb per million (RPKM) gene expression values, genes with average $\log_2$ RPKM of 2 or more in at least one group were considered expressed above detection threshold. Using this selection threshold, 17,901 genes were included in the downstream analysis.

Transcriptomics weighted correlation network analysis. WGCNA was performed using CQN and $\log_2$-transformed RPKM values. Based on the relationship between power and scale independence, the power of 6 was chosen to build scale-free topology using unsigned network (3). Hybrid dynamic tree cutting was utilized based on a minimum module size of 60 genes and a minimum height for merging modules of 0.4. Each module was summarized by module eigengene. Each module was assigned a unique color identifier, and genes that did not fulfil criteria for any of the modules were assigned to the gray module. Modules markedly associated with a group were annotated using WGCNA R function GOenrichmentAnalysis. Genes with high connectivity in the respective modules were considered hub genes. Intra-modular gene-gene connection was visualized using VisANT.

qRT-PCR. Total RNAs were extracted from the samples using an RNeasy mini kit with DNase (QIAGEN). In the case of brains, samples were treated with TRIzol RNA Isolation Reagents (Thermo Fisher Scientific, 15596026) prior to extraction. Reverse transcription with total RNA was performed using an iScript cDNA synthesis kit (BioRad, 1708891). The following primers were purchased from Integrated DNA Technologies, Inc.; *Tnf* F 5′-AGCCCACGTCGTAGCAAACCAC-3′, R 5′-AGGTACAACCCATCGGCTGGCA-3′; *Il1b* F 5′-CCTGCAGCTGGAGAGTGTGGAT-3′, R 5′-TGTGCTCTGCTTGTGAGGTGCT-3′; *Il6* F 5′-TCCTTAGCCACTCCTTCTGT-3′, R 5′- AGCCAGAGTCCTTCAGAGA-3′; *Cd14* F 5′-

AAAGAAACTGAAGCCTTTCTCG-3′, R 5′-AGCAACAAGCCAAGCACAC-3′; *Abca7* F 5′-ACACACAGACACGCCACCT-3′, R 5′-CATGATGACCACACGAGAGC-3′; *Apoe* F 5′-ACAGAT CAGCTCGAGTGGCAAA-3′, R 5′-ATCTTGCGCAGGTGTGTGGAGA-3′; *Trem2* F 5′-GCACCTCCAGGAATCAAGAG-3′, R 5′-GGGTCCAGTGAGGATCTGAA-3′; *Cx3cr1* F 5′-CAGCATCGACCGGTACCTT-3′, R 5′-GCTGCACTGTCCGGTTGTT-3′; *Tmem119* F 5′-ATAGCTCAACATGGTCCCCTGGTTC-3′, R 5′-GGCCTGTTAGACACTGGGGGAGAC-3′; *Hprt* F 5′-TCCTCCTCAGACCGCTTTT-3′, R 5′-CCTGGTTCATCATCGCTAATC-3′ and *Hexb*, Mm.PT.58.5088062. Quantitative PCR reaction with SsoAdvanced Universal SYBR Green Supermix (BioRad, 1725271) was performed using Quantstudio 7 (Thermo Fisher Scientific).

Western blotting. Microglia were collected using an 11-mm fixed-blade scraper (USA Scientific, CC7600-0220) after washing with phosphate-buffered saline (PBS), and dissolved in T-PER (Thermo Fisher Scientific, 78510) containing phosphatase (PhosSTOP, Roche, 4906845001) and protease inhibitor cocktails (Complete EDTA-free Protease Inhibitor cocktail, Roche, 11873580001). Brain samples were suspended in T-PER containing a protease inhibitor cocktail after washing with PBS, and homogenized with a polytron homogenizer (EYELA model PT1200E). The protein concentrations of soluble supernatants were measured with a BCA protein assay kit (Thermo Fisher Scientific, 23225), and the lysates (10-50 μg) were subjected to SDS-PAGE, followed by electrotransfer to the PVDF membrane (Immobilon PVDF transfer membrane, EMD Millipore, IP00010). After incubation with antibodies, immunoreactivities were detected and quantified using Odyssey Infrared Imaging System (LI-COR Biosciences). The following primary antibodies were used: rat monoclonal antibody against mouse ABCA7 (clone MABI 97-17, produced at MAB Institute) (4), GAPDH (Santa Cruz biotechnologies, 6C5), NF-kB p65 (Cell Signaling Technologies, clone L8F6), phospho-NF-kB p65 (Ser536) (Cell Signaling Technologies, clone 93H1), MAPK-p38 (Cell Signaling Technologies, 9212S), phospho-MAPK-p38 (Cell Signaling Technologies, clone D3F9, 4511T), ERK1/2 (Cell Signaling Technologies, clone L34F12, 4696S), and phospho-ERK1/2 (Cell Signaling Technologies, clone D13.14.4E, 4370T).

Enzyme-Linked Immunosorbent Assay. Mouse brains were lysed through a three-step extraction method using Tris-buffered saline (TBS), TBS containing 1% Triton X-100 (TBS-X), and 5M guanidine hydrochloride (GDN-HCl). Amounts of Aβ40 and Aβ42 in each fraction were determined by enzyme-linked immunosorbent assay (ELISA) as previously described (5). Colorimetric changes were measured through a Synergy HT plate reader (BioTek) and quantified based on the standard curve. Each value was normalized against total protein amount determined by BCA protein assay.

Aβ42 internalization in primary microglia. Primary microglia was incubated with serum free DMEM for 2 hours, and then changed to 500 nM FAM-Aβ1-42 (ANASPEC, Beta-Amyloid (1-42), FAM-labeled, Human, AS-23526) in FBS containing DMEM for 1.5 hours. After incubation, cells were fixed with 4% paraformaldehyde, and stained with EEA1, Rab7 and LAMP1 antibodies. Images were obtained using confocal laser-scanning fluorescence microscopy. Image J was used for counting signals. And the JACoP plugin in Image J was used for co-localization of signals.

Supplementary Table 1. Enriched genes in modules for cortical transcripts from control and *Abca7*$^{+/-}$ mice with or without LPS administration

Module Color	Gene	GS.group	p.GS.group	MM.module	p.MM.module
Turquoise	***Cd14***	–0.901	1.84E-09	–0.989	1.00E-19
Turquoise	***Akap12***	–0.901	1.96E-09	–0.988	2.59E-19
Turquoise	***Pnp***	–0.885	9.24E-09	–0.988	2.95E-19
Turquoise	***Errfi1***	–0.887	7.59E-09	–0.988	3.44E-19
Turquoise	***Mt2***	–0.884	9.78E-09	–0.986	9.14E-19
Turquoise	***Plaur***	–0.878	1.78E-08	–0.986	9.44E-19
Turquoise	***Clic4***	–0.905	1.23E-09	–0.986	1.83E-18
Turquoise	***Bach1***	–0.896	3.22E-09	–0.985	2.29E-18
Turquoise	***Hck***	–0.878	1.79E-08	–0.985	2.48E-18
Turquoise	***Jcad***	0.890	6.14E-09	0.985	2.64E-18
Blue	***Slc17a6***	–0.553	0.00511	–0.961	9.46E-14
Blue	***Trpv6***	0.491	0.01487	0.959	1.49E-13
Blue	***Plcb4***	–0.668	0.00036	–0.958	1.94E-13
Blue	***Slc6a11***	–0.590	0.00239	–0.957	2.73E-13
Blue	***Unc13b***	0.706	0.00012	0.954	5.79E-13
Blue	***Rasgef1a***	0.729	0.00005	0.950	1.26E-12
Blue	***Chn1os3***	0.680	0.00026	0.949	1.55E-12
Blue	***Itpkb***	–0.511	0.01076	–0.949	1.58E-12
Blue	***Sparc***	–0.468	0.02117	–0.949	1.70E-12
Blue	***Kcnh4***	0.566	0.00393	0.948	2.09E-12
Light cyan	***Daam2***	–0.553	0.005	0.921	1.81E-10
Light cyan	***Mxd4***	–0.591	0.002	0.910	7.39E-10
Light cyan	***Cbs***	–0.542	0.006	0.908	9.36E-10
Light cyan	***Mfsd2a***	–0.445	0.029	0.907	1.05E-09
Light cyan	***Nde1***	–0.481	0.017	0.902	1.77E-09
Light cyan	***Phyhd1***	–0.395	0.056	0.897	3.03E-09
Light cyan	***Cdh19***	–0.423	0.039	0.888	6.93E-09
Light cyan	***Lmna***	0.489	0.015	–0.882	1.23E-08
Light cyan	***Acot11***	–0.456	0.025	0.872	2.93E-08
Light cyan	***Fzd2***	–0.517	0.010	0.870	3.24E-08
Light cyan	***Htra1***	–0.296	0.160	0.868	3.83E-08
Light cyan	***Pak7***	0.391	0.059	–0.866	4.63E-08

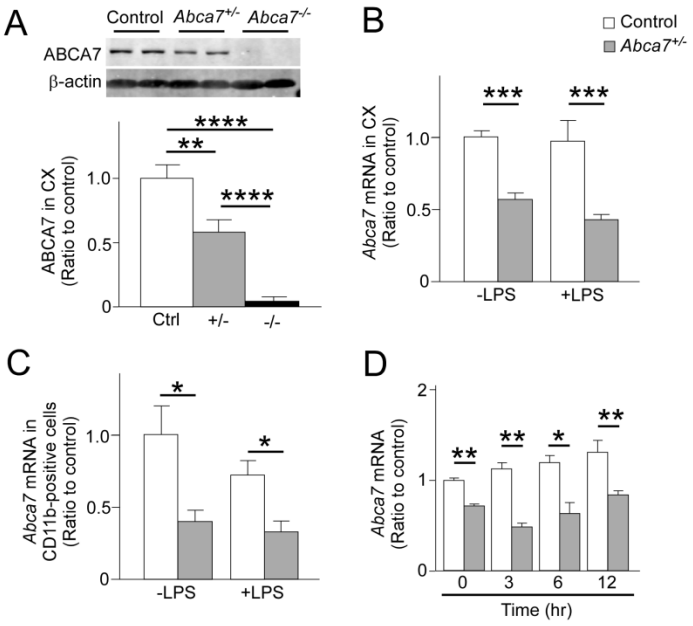

Supplementary figure 1. ABCA7 expression in heterozygous *Abca7* knockout mice after LPS stimulation. (A) ABCA7 levels in the cortex (CX) from control (white), *Abca7*$^{+/-}$ (gray), and *Abca7*$^{-/-}$ (black) mice were analyzed by Western blotting (control; N=3, *Abca7*$^{+/-}$; N=3, *Abca7*$^{-/-}$; N=3). (B) *Abca7* mRNA expression was analyzed in the CX of mice 3.5 hours after administration with (control; N=9, *Abca7*$^{+/-}$; N=9) or without (control; N=6, *Abca7*$^{+/-}$; N=6) intraperitoneal LPS injection. (C) CD11b-positive microglia was isolated from the CX of the mice 7 hours after administration with (control; N=9, *Abca7*$^{+/-}$; N=9) or without (control; N=4, *Abca7*$^{+/-}$; N=4) intraperitoneal LPS injection, and *Abca7* mRNA levels were measured. (D) *Abca7* mRNA expression in primary microglia from the mice was assessed 3, 6, and 12 hours after LPS administration (N=3/each). The ΔΔCt values of *Abca7* relative to *Hprt* were measured by qRT-PCR. Relative ratios to control mice or microglia without LPS administration are shown as mean ± SEM. **P*<0.05, ***P*<0.01, ****P*<0.001, *****P*<0.0001, by Student *t* test at each time point (A, D) or Tukey-Kramer post-hoc analysis of two-way ANOVA (B, C).

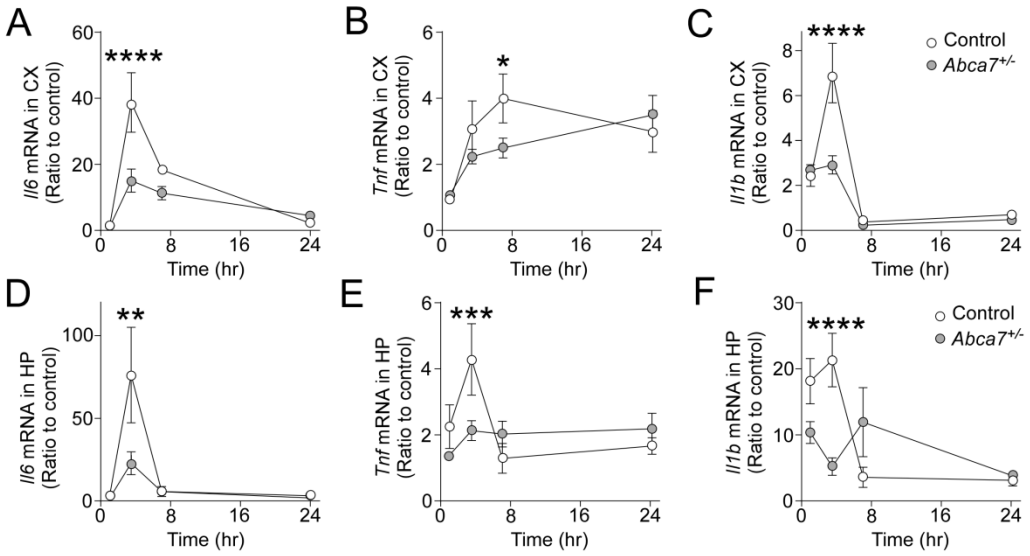

Supplementary figure 2. Time-dependent expression of inflammatory cytokine in the brains of heterozygous *Abca7* knockout mice upon peripheral LPS administration. The mRNA expressions of inflammatory cytokines were analyzed in the cortex (CX; A-C) and hippocampus (HP; D-F) of control (white) and *Abca7*$^{+/-}$ (gray) mice 1 (control; N=4, *Abca7*$^{+/-}$; N=4), 3.5 (control; N=15, *Abca7*$^{+/-}$; N=17), 7 (control; N=4, *Abca7*$^{+/-}$; N=4), and 24 (control; N=4, *Abca7*$^{+/-}$; N=4) hours after intraperitoneal LPS injection. Some results from Fig. 1A-F were incorporated into the time point at 3.5 hours after injection. The ΔΔCt values of *Il6* (A, D), *Tnf* (B, E), and *Il1b* (C, F) relative to *Hprt* were measured by qRT-PCR. Relative ratios to control mice without LPS administration are shown as mean ± SEM. **P*<0.05, ***P*<0.01, ****P*<0.001, *****P*<0.0001 by Student *t* test at each time point.

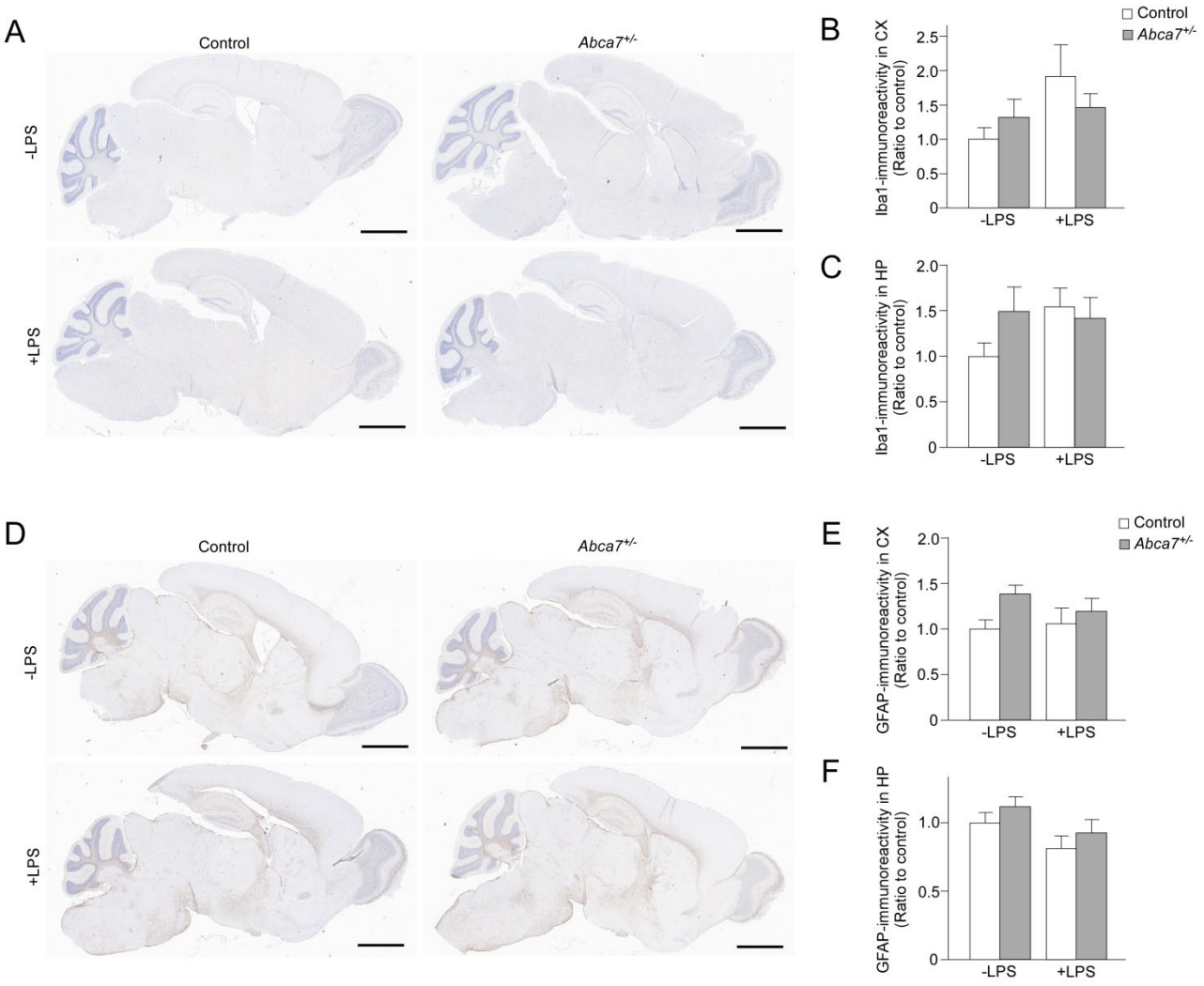

Supplementary figure 3. Influences of ABCA7 haplodeficiency on glial activation after peripheral LPS administration. Brain sections from control and *Abca7*$^{+/-}$ mice were immunostained for Iba-1 (A-C) and GFAP (D-F) 3.5 hours after administration (control; N=5, *Abca7*$^{+/-}$; N=5) or without (control; N=6, *Abca7*$^{+/-}$; N=5) intraperitoneal LPS injection. Scale bars: 1 mm. Immunoreactivity for Iba-1 and GFAP in the cortex (CX; B, E) and hippocampus (HP; C, F) are quantified through the Positive Pixel Count program using Aperio Technologies. Relative ratios to control mice without LPS administration (CX) are shown as mean ± SEM. Not significant by Tukey-Kramer post-hoc analysis of two-way ANOVA.

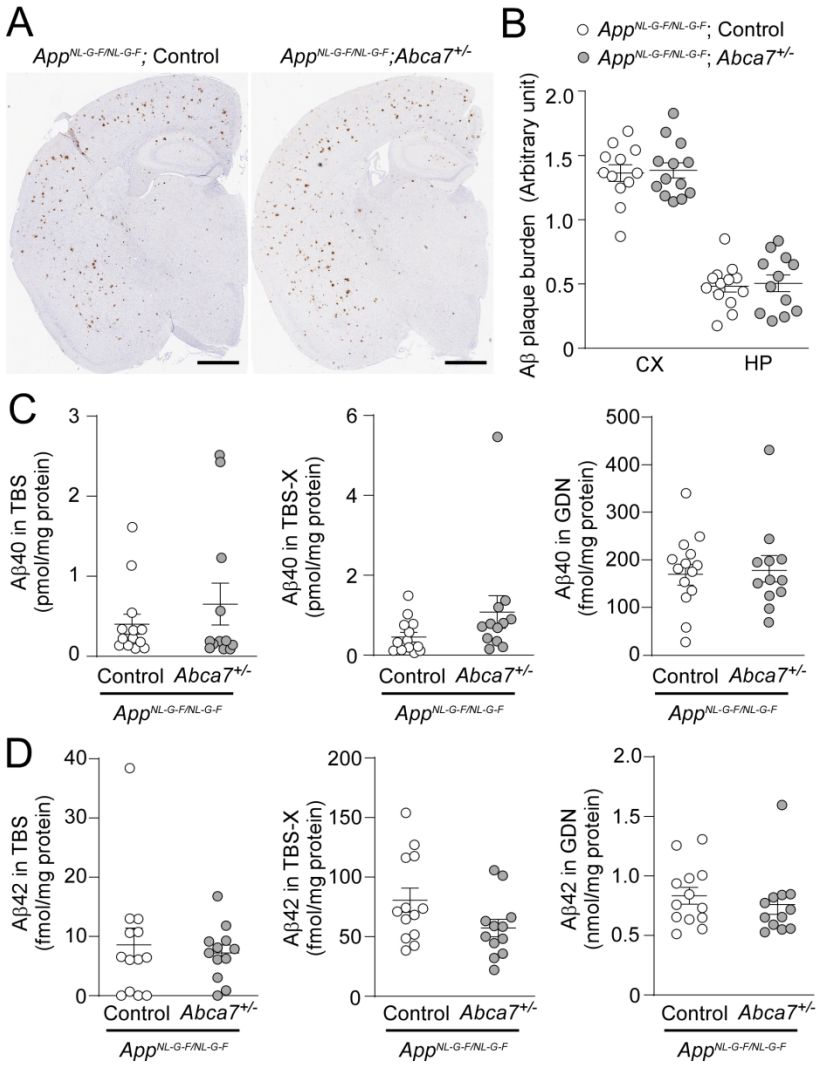

Supplementary figure 4. Aβ pathology in *App*$^{NL\text{-}G\text{-}F/NL\text{-}G\text{-}F}$; *Abca7*$^{+/-}$ mice. (A) Brain sections from *App*$^{NL\text{-}G\text{-}F/NL\text{-}G\text{-}F}$; Control (N=13) and *App*$^{NL\text{-}G\text{-}F/NL\text{-}G\text{-}F}$; *Abca7*$^{+/-}$ mice (N=12) were immunostained with pan-Aβ antibody at the age of 3 months. Scale bars: 1 mm. (B) Amyloid plaque burdens in the cortex (CX) and hippocampus (HP) were quantified through the Positive Pixel Count program using Aperio Technologies. (C, D) The concentrations of Aβ40 (C) and Aβ42 (D) in CX extracted in TBS, TBS-X, and GDN-HCl fractions from the mice were measured by ELISA at 3 months of age. Relative ratios to *App*$^{NL\text{-}G\text{-}F/NL\text{-}G\text{-}F}$; Control mice (CX) are shown as mean ± SEM. Not significant by Student *t* test or Wilcoxon test.

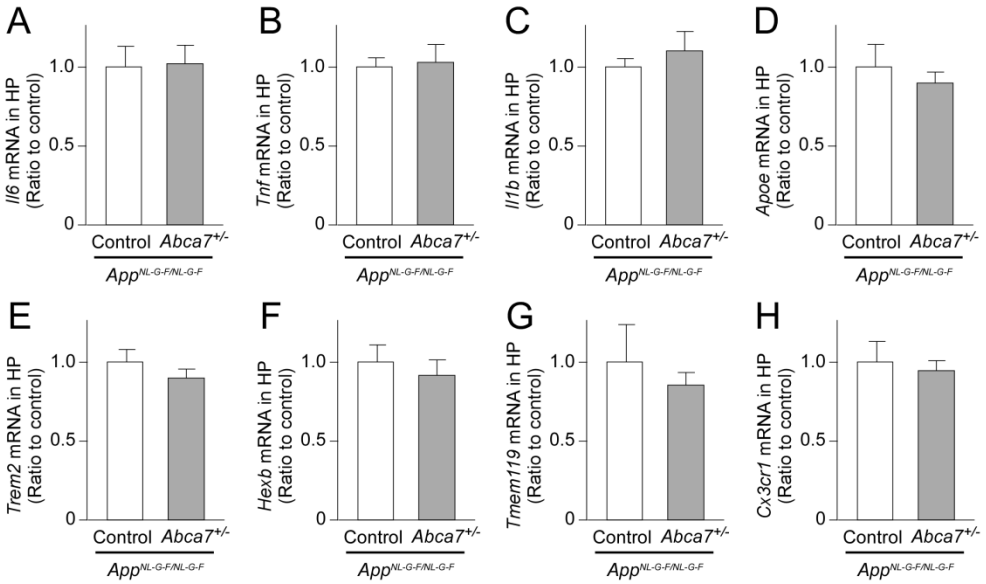

Supplementary figure 5. Inflammatory cytokine expressions in the hippocampus of *App*$^{NL\text{-}G\text{-}F/NL\text{-}G\text{-}F}$; *Abca7*$^{+/-}$ mice. The mRNA expressions of inflammatory cytokines and disease-associated microglia markers were analyzed in the hippocampus (HP) of *App*$^{NL\text{-}G\text{-}F/NL\text{-}G\text{-}F}$; Control (N=13) and *App*$^{NL\text{-}G\text{-}F/NL\text{-}G\text{-}F}$; *Abca7*$^{+/-}$ mice (N=12). The ΔΔCt values of *Il6* (A), *Tnf* (B), *Il1b* (C), *Apoe* (D), *Trem2* (E), *Hexb* (F), *Tmem119* (G), and *Cx3cr1* (H) relative to *Hprt* were measured by qRT-PCR. Relative ratios to control mice are shown as mean ± SEM. Not significant by Student *t* test or Wilcoxon test.

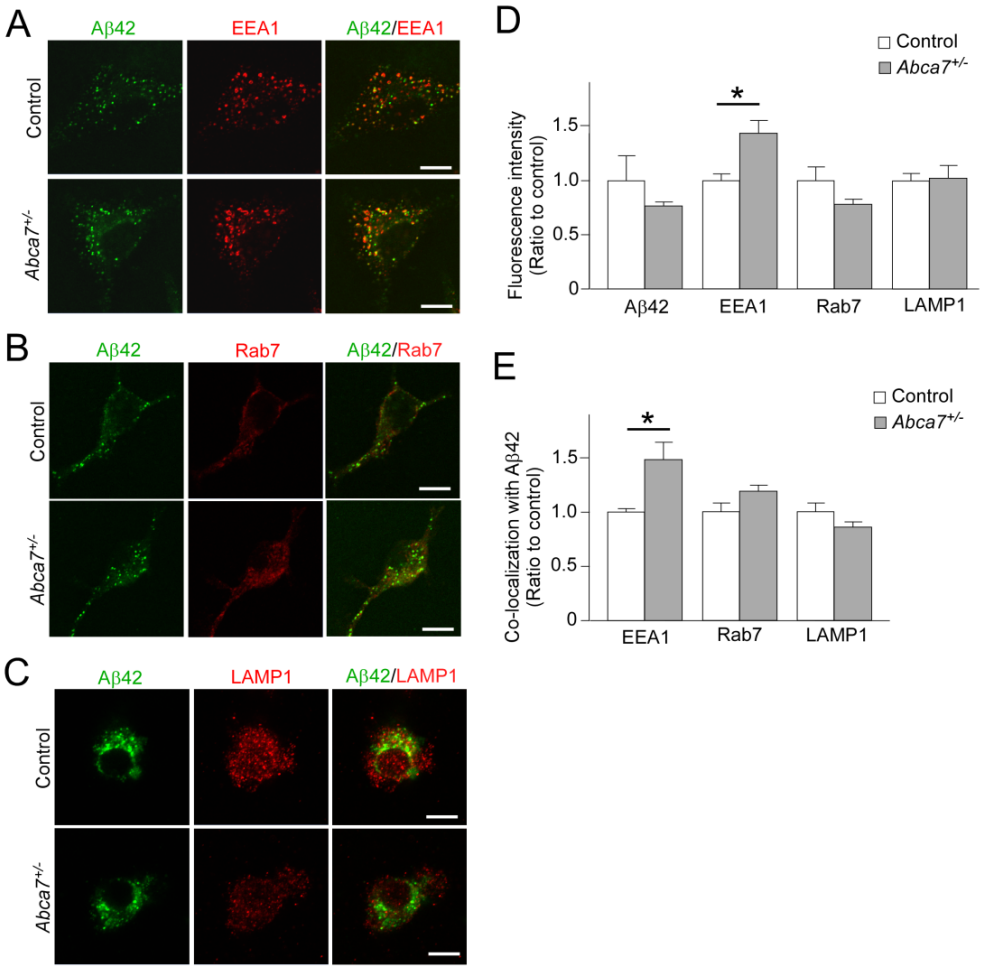

Supplementary figure 6. Cellular internalization of Aβ42 in primary microglia. Primary cultures of microglia from control and *Abca7*$^{+/-}$ mice were incubated with FAM-Aβ42. Scale bars = 5 μm. After incubation with FAM-Aβ42, microglia was immunostained for EEA1 (A), Rab7 (B) or LAMP1 (C). Images were acquired through the confocal microscopy and their fluorescence intensities in microglia were quantified by Image J (D). Co-localizations of FAM-Aβ42 with EEA1-, Rab7- or LAMP1-positive compartments were quantified by Image J (E). Relative ratios to control microglia are shown as mean ± SEM (N=3/each). *P<0.05 by Student's *t* test.

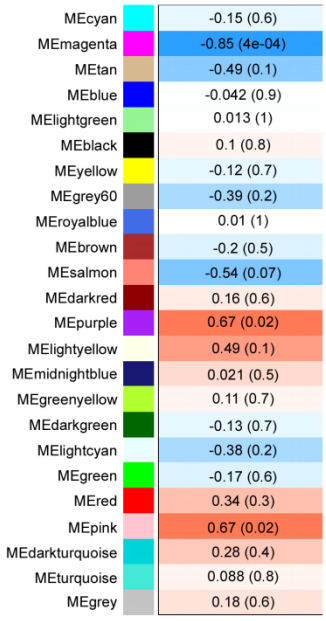

Module color	Rank	Enrichment p value	ID	GO process
pink	1	4.28E-04	GO:0007009	plasma membrane organization
pink	2	5.34E-04	GO:0010256	endomembrane system organization
pink	3	9.19E-04	GO:0043651	linoleic acid metabolic process
pink	4	1.36E-03	GO:0006480	N-terminal protein amino acid methylation
pink	5	1.36E-03	GO:0035902	response to immobilization stress
pink	6	1.36E-03	GO:0018542	2,3-dihydroxy DDT 1,2-dioxygenase activity
pink	7	1.36E-03	GO:0018555	phenanthrene dioxygenase activity
pink	8	1.36E-03	GO:0018556	2,2',3-trihydroxybiphenyl dioxygenase activity
pink	9	1.36E-03	GO:0018557	1,2-dihydroxyfluorene 1,1-alpha-dioxygenase activity
pink	10	1.36E-03	GO:0018558	5,6-dihydroxy-3-methyl-2-oxo-1,2-dihydroquinoline dioxygenase activity
purple	1	5.56E-04	GO:0017099	very-long-chain-acyl-CoA dehydrogenase activity
purple	2	9.51E-04	GO:0004466	long-chain-acyl-CoA dehydrogenase activity
purple	3	9.64E-04	GO:0030103	vasopressin secretion
purple	4	9.64E-04	GO:0008241	peptidyl-dipeptidase activity
purple	5	1.16E-03	GO:0000077	DNA damage checkpoint
purple	6	1.49E-03	GO:0046322	negative regulation of fatty acid oxidation
purple	7	2.18E-03	GO:0008349	MAP kinase kinase kinase kinase activity
purple	8	2.46E-03	GO:0004180	carboxypeptidase activity
purple	9	2.74E-03	GO:0050660	flavin adenine dinucleotide binding
purple	10	2.83E-03	GO:0046813	receptor-mediated virion attachment to host cell
magenta	1	1.17E-04	GO:2000507	positive regulation of energy homeostasis
magenta	2	2.55E-04	GO:0046886	positive regulation of hormone biosynthetic process
magenta	3	4.82E-04	GO:0035162	embryonic hemopoiesis
magenta	4	6.00E-04	GO:0045940	positive regulation of steroid metabolic process
magenta	5	7.19E-04	GO:0060706	cell differentiation involved in embryonic placenta development
magenta	6	8.30E-04	GO:0050790	regulation of catalytic activity
magenta	7	8.85E-04	GO:0043085	positive regulation of catalytic activity
magenta	8	9.64E-04	GO:0001575	globoside metabolic process
magenta	9	9.64E-04	GO:0051597	response to methylmercury
magenta	10	9.64E-04	GO:0004103	choline kinase activity

Supplementary figure 7. Altered cortical transcriptome by ABCA7 haplodeficiency. Transcriptome in the cortex of male control and *Abca7*$^{+/-}$ mice when analyzed through RNA-sequencing (N=6/each). Each module is determined based on topological overlap through WGCNA among the two groups of mice: 1) control and 2) *Abca7*$^{+/-}$ mice. Each module is assigned with a unique color, and the module traits are correlated with two mouse groups (1 to 2). The corresponding correlations and *P* values are displayed for each module. Modules with significant change ($P \leq 0.05$) were analyzed for pathway enrichment.

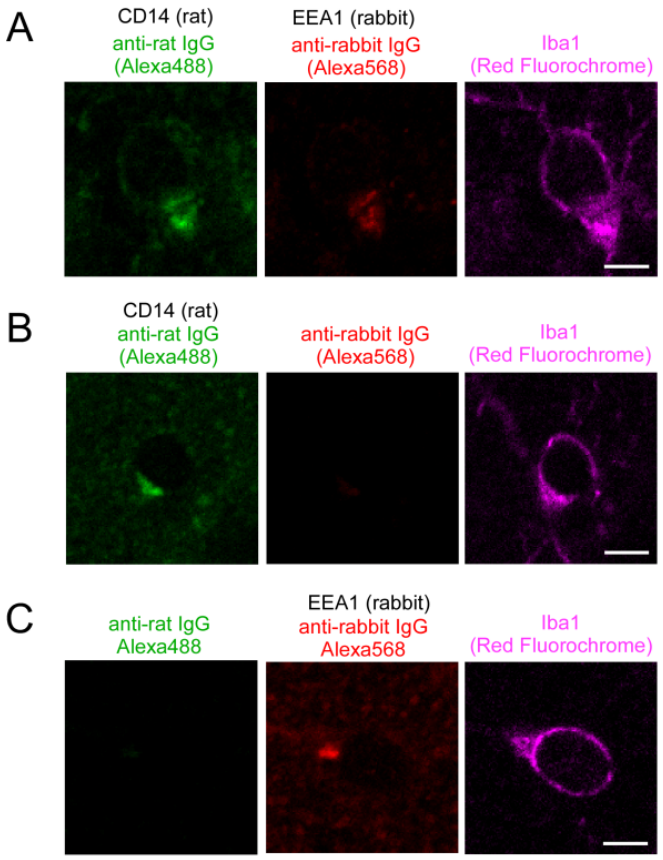

Supplementary figure 8. Triple immunofluorescence staining with antibodies for CD14, EEA1 and Iba1. (A) Brain sections from *App*$^{NL\text{-}G\text{-}F/NL\text{-}G\text{-}F}$ were immunostained with anti-CD14 rat antibody and anti-rat IgG secondary antibody conjugated with Alexa488 (green) and anti-EEA1 rabbit antibody and anti-rabbit IgG secondary antibody conjugated with Alexa568 (red), followed by Red Fluorochrome-conjugated Iba1 antibody (magenta). (B, C) To assess the possibility for cross-reactivity of antibodies and bleed-through of fluorescence emission, the brain sections were similarly stained in the condition without primary EEA antibody (B) or CD14 antibody (C). Scale bars = 5 μm.

1. M. Nikodemova, J. J. Watters, Efficient isolation of live microglia with preserved phenotypes from adult mouse brain. *J Neuroinflamm* **9**, 147 (2012).
2. Y. Ren *et al.*, TMEM106B haplotypes have distinct gene expression patterns in aged brain. *Mol Neurodegener* **13**, 35 (2018).
3. M. Matarin *et al.*, A genome-wide gene-expression analysis and database in transgenic mice during development of amyloid or tau pathology. *Cell Rep* **10**, 633-644 (2015).
4. N. Iwamoto, S. Abe-Dohmae, R. Sato, S. Yokoyama, ABCA7 expression is regulated by cellular cholesterol through the SREBP2 pathway and associated with phagocytosis. *J Lipid Res* **47**, 1915-1927 (2006).
5. N. Sakae *et al.*, ABCA7 Deficiency Accelerates Amyloid-beta Generation and Alzheimer's Neuronal Pathology. *J Neurosci* **36**, 3848-3859 (2016).